Original Article

High Performance Polymers

High Performance Polymers
1–10

DOI: 10.1177/0954008320967052
journals.sagepub.com/home/hip

Soluble and transparent polyimides with high T_gs from a new semi-aliphatic diamine with cyclohexyl and ortho-methyl groups

Xiaoqian He[1], Shoubai Wang[2], Xiuming Wu[1], Chen Shu[1], Xiang Fan[3], Zhenhai Yu[3] and Wei Huang[1]

Abstract

Herein a semi-aliphatic diamine 4,4′-(cyclohexylmethylene)bis(2-methylaniline) (CHMBMA) with a pendant cyclohexyl and two ortho-substituted methyl groups is synthesized from o-toluidine and cyclohexanecarbaldehyde by Mannich and rearrangement reactions. Then CHMBMA is polycondensed with five commercial aromatic dianhydrides by the high-temperature one-step method with the thermal imidization to produce a series of polyimides (PIs, PI-H(1–5)). The weight-averaged molecular weights (M_ws) of PI-H(1–5) are in the range from 9.08×10^4 to 27.48×10^4 g mol^{-1} with the polydispersity indices (PDI) from 3.29 to 6.13 by gel permeation chromatography (GPC) measurement. They are soluble in common organic solvents (such as THF, $CHCl_3$ etc.) and can form transparent, tough films with light-color (Thickness: 20–26 μm) by the solution-casting method. The light transmittance of them is above 80% in the visible range from 400 to 760 nm. They exhibit excellent mechanical properties with tensile strength from 72.2 to 97.06 MPa and tensile modulus from 0.9 to 1.9 GPa. Furthermore, they also display low water absorption rates (<2.5%), good thermal stability (5% weight loss temperatures ($T_{5\%}$) in the range from 466 to 480°C under N_2 atmosphere and high glass transition temperatures (T_gs $\geq$ 319°C). As comparison, we also synthesize these PIs (PI-L(1–5)) by the low-temperature two-step method with the chemical imidization. The M_ws of PI-L(1–5) are lower than those of PI-H(1–5), but the film color of PI-L(1–5) is relatively lighter than the corresponding one of PI-H(1–5). In summary, the introduction of cyclohexyl and ortho-substituted methyl groups into the backbone can improve the solubility of PIs and the transparency of their corresponding films without reducing their T_gs.

Keywords

Cyclohexyl, film, ortho-substituted methyl, polyimide, transparency

Introduction

Polyimides, basically synthesized from an electron donating diamine and an electron accepting dianhydride, usually possess many outstanding properties (e.g., high mechanical properties, low dielectric constants, excellent thermal stability etc.) and attract much attention in the fields of science and industry.[1–4] Unfortunately, the rigid backbones of conventional aromatic PIs often result in the difficult processing of them in solution or molten state. In addition, it is easy to form intramolecular and intermolecular charge-transfer complex (CTC) that usually causes the low transparency and deep color of PI films.[5–10] These two drawbacks impede the applications of PIs in microelectronic and optoelectronic engineering.[11,12] Therefore, lots of efforts have been made to overcome above-mentioned problems through the design and modification of PI molecular structures,[13] including introduction of bulky pendent groups (e.g., cyclobutyl and cyclohexyl) to decrease close-packing and intermolecular CT interactions,[14–16] flexible linkages (e.g., –O–, $–CH_2–$ and –S–) to provide kinks in the polymer backbones,[17–19]

[1] School of Chemistry and Chemical Engineering, State Key Laboratory of Metal Matrix Composites, Shanghai Key Laboratory of Electrical Insulation and Thermal Aging, Shanghai Jiao Tong University, Shanghai, China
[2] Nantong University Xinglin College, Nantong, China
[3] Shanghai Institute of Space Power-Sources, Shanghai, China

Corresponding authors:
Wei Huang, School of Chemistry and Chemical Engineering, State Key Laboratory of Metal Matrix Composites, Shanghai Key Laboratory of Electrical Insulation and Thermal Aging, Shanghai Jiao Tong University, 800 Dongchuan Road, Shanghai 200240, China.
Email: hw66@sjtu.edu.cn

Shoubai Wang, Nantong University Xinglin College, 9 Seyouan Road, Nantong 226019, China.
Email: swang@ntu.edu.cn

noncoplanar structures to reduce crystallinity and hinder interactions,[20–22] and fluorine substituents like trifluoromethyl or perfluoro groups to weaken intermolecular cohesive force and reduce CTC formation.[23–27] However, the approaches to enhance transparency or solubility of PIs are usually contradicted with the demand to keep their good inherent properties, such as excellent mechanical properties, thermal stability and so on.[28–30] Fortunately, it is considered an effective way that incorporating bulky pendant groups into PIs to improve their processability and transparency, and meanwhile maintain their high thermal stability.[31–34] In previous work, we found that the introduction of cyclohexyl and *tert*-butyl groups into PIs was able to increase their T_gs, solubility and transparency,[34] but the cost was relatively high. In order to decrease the cost and further enhance the T_gs of PIs, we intend to use methyl instead of *tert*-butyl.[3,35]

Herein, a new semi-aliphatic diamine 4,4′-(cyclohexylmethylene)bis(2-methylaniline) with cyclohexyl and ortho-substituted methyl groups was designed and synthesized through Mannich and rearrangement reactions. Then a series of soluble and transparent PIs with high T_gs were prepared from CHMBMA and five commercial aromatic dianhydrides via the high-temperature one-step method. As comparison, they were also synthesized by the low-temperature two-step method. The resulting PIs and their corresponding films were investigated and discussed in detail as follows.

Experimental

Materials

O-toluidine (Beijing Inokai Technology Co. Ltd.) and m-cresol (Shanghai Macklin Biochemical Co. Ltd.) were purified by the vacuum distillation before use. Pyromellitic dianhydride (PMDA, Sinopharm Chemical Reagent Co. Ltd.), 2,2-bis(3,4-dicarboxyphenyl)-1,1,1,3,3,3-hexafluoropropane dianhydride (6FDA, Shanghai Titan Scientific Co. Ltd.), 3,3′,4,4′-diphenylether tetracarboxylic dianhydride (ODPA, Adamas Reagent Co. Ltd), 3,3′,4,4′-biphenyltetracarboxylic dianhydride (BPDA, Adamas Reagent Co. Ltd), and 3,3′,4,4′-benzophenone-tetracarboxylic dianhydride (BTDA, J&K Chemical Co. Ltd.) were purified by recrystallization from acetic anhydride before use. Cyclohexanecarboxaldehyde (Adamas Reagent Co. Ltd), isoquinoline (Shanghai Titan Scientific Co. Ltd), hydrochloric acid (Sinopharm Chemical Reagent Co. Ltd.), dry N-methylpyrrolidone (NMP, Adamas Reagent Co. Ltd), pyridine (Adamas Reagent Co. Ltd), acetic anhydride (Shanghai Titan Scientific Co. Ltd) and other materials were used as received.

Measurements

The ^{1}H and ^{13}C NMR measurements of diamine CHMBMA were performed on a 400 MHz Bruker NMR spectrometer with DMSO-d_6 as a solvent. The ^{1}H and ^{13}C NMR spectra of the resulting PIs were obtained by a 500 MHz Bruker NMR spectrometer with $CDCl_3$ as a solvent. The spectra of liquid chromatography-mass spectrometer (LC-MS) and high resolution mass spectrometer (HRMS) were determined by ACQUITYTM UPLC & Q-TOF MS Premier. The FTIR spectra were carried out on a Perkin-Elmer Fourier transform infrared spectrometer. The molecular weights were measured with a Perkin-Elmer series 200 gel permeation chromatography (GPC) analyzer (polystyrene calibration), using DMF as eluent containing 0.02 M LiBr (0.6 mL min^{-1}). Elemental analysis was performed on a vario EL cube elemental analyzer. The mechanical behaviors of the PI films were performed by using an INSTRON 4465 tensile tester at a drawing speed of 1 mm min^{-1}. The optical performance of the PI films was obtained on a Perkin-Elmer Lambda 20 UV-Vis spectrometer for a thickness of 20–26 μm. The X-ray diffraction (XRD) measurement was investigated on a Bruker D8 advance X-ray diffractometer using Cu/K-α radiation with 2θ in the range from 5 to 50°. The water absorption rates of PI films were investigated according to the weight changes of PI films before and after immersing in deionized water at 25°C for 72 h. Thermogravimetric analysis (TGA) was carried out by a TA Discovery TGA Q5000 thermal analyzer under N_2 condition at a heating rate of 20°C min^{-1} from 50°C to 800°C. Differential scanning calorimetry (DSC) curves were measured on a TA Discovery DSC 2500 thermal analyzer under N_2 atmosphere at a heating rate of 10°C min^{-1} from 40°C to 400°C. Dynamic mechanical analyzer (DMA) was obtained by a DMA Q800 (TA Instruments) thermal analysis system with a heating rate of 5°C min^{-1} and a load frequency of 1 Hz under N_2 atmosphere. The thermal expansion coefficients (CTE) of PI films (15 mm × 6 mm × 40 μm) were measured by thermomechanical analysis (TMA) on a Mettler Toledo TMA/SDTS841e thermal analyzer system under N_2 condition at a heating rate of 10°C min^{-1} from 50°C to 200°C with 0.02 N expansion force.

Synthesis of CHMBMA

The synthetic route of CHMBMA is illustrated in Figure 1. O-Toluidine (53.5368 g, 0.5 mol) and 36–38 wt% hydrochloric acid (9.7 mL, 0.1 mol) were added into a 250 mL three-necked flask equipped with a reflux condenser and a stirring bar under N_2 atmosphere. Firstly, the mixture was stirred for 0.5 h at room temperature and then heated at 100°C for 2 h. Secondly, cyclohexanecarbaldehyde (22.4344 g, 0.2 mol) was added into the flask under the stirring and maintained at 100°C for 10 h. Thirdly, 28–30 wt% aqueous ammonia (13.4 mL, 0.2 mol) and 30 mL CH_2Cl_2 were added into the mixture under the vigorous stirring for 0.5 h after it was cooled to room temperature. Then the mixture was washed with deionized water (50 mL * 3) and the CH_2Cl_2 solution containing crude product was obtained by a separatory funnel. It was concentrated by a rotary

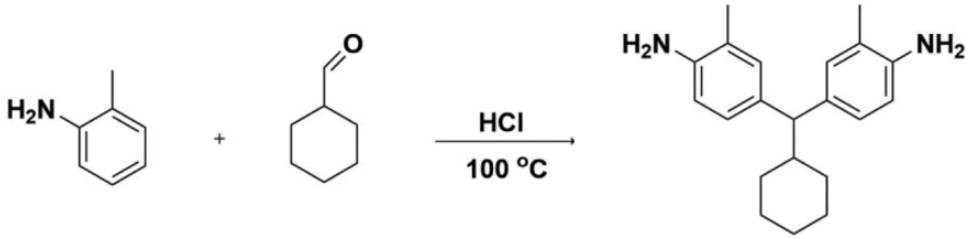

Figure 1. Synthesis of semi-aliphatic diamine CHMBMA.

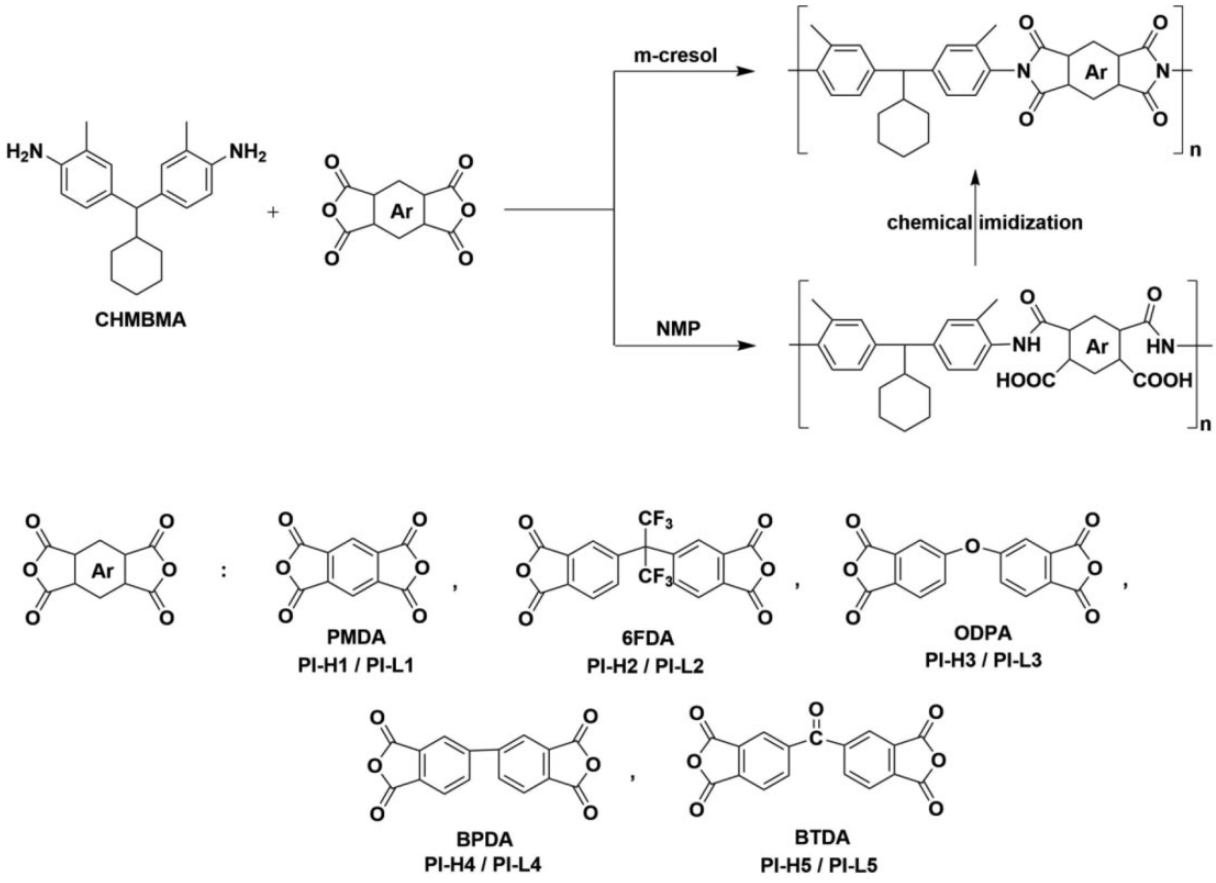

Figure 2. Synthesis of PI-H(1–5) and PI-L(1–5) via high-temperature one-step method and low-temperature two-step method.

evaporator under reduced pressure to produce some yellow oily product. Finally, some light yellow solid was obtained by vacuum distillation to collect the fraction with the boiling range from 210 to 215°C (20 Pa). Then it was recrystallized in anhydrous ethanol and 20.976 g white crystal was obtained after drying in vacuum at 60°C. Yield: 34%; m.p.:121°C; ^{1}H NMR (400 MHz, DMSO-d6) δ 6.80 (d, J = 7.2 Hz, 4H), 6.52–6.47 (m, 2H), 4.52 (s, 4H), 3.08 (d, J = 10.9 Hz, 1H), 2.01 (s, 6H), 1.94 (d, J = 10.8 Hz, 1H), 1.64–1.51 (m, 5H), 1.22–1.07 (m, 3H), 0.76 (q, J = 10.8, 10.3 Hz, 2H). ^{13}C NMR (101 MHz, DMSO-d6) δ 144.44, 133.76, 129.85, 125.87, 121.27, 114.46, 57.64, 41.13, 32.31, 26.73, 26.28, 18.08. HRMS (ESI, *m/z*): $[M+H]^+$ calcd for $C_{21}H_{28}N_2^+$, 309.2331; found, 309.2347.

Synthesis of PIs

High-temperature one-step method. PI-H(1–5) were prepared by a high-temperature one-step method as shown in Figure 2. As as a typical example, **PI-H1** was synthesized according to the following procedure. 1.5423 g (5 mmol) CHMBMA, 1.0906 g (5 mmol) PMDA, 15 mL *m*-cresol and 10 drops isoquinoline were added into a 100 mL three-necked flask equipped with a mechanical stir, a reflux condenser and a nitrogen inlet. Then the mixture was stirred at room temperature for 1 h under N_2 atmosphere and further heated in turn at 50°C for 12 h, 80°C for 12 h, 150°C for 12 h and 180°C for 12 h. After cooling to room temperature, the viscous yellow mixture was diluted by adding 30 mL

chloroform and then poured slowly into 500 mL methanol under the vigorous stirring to give some white fiber-like precipitate. Finally, PI-H1 was collected by filtration and dried at 150°C in vacuum oven for 24 h. It was purified by reprecipitating twice. Yield: 94%. FTIR (blade-coating film, cm^{-1}): ν = 2928 (CH_2–H), 1779 (C=O), 1728 (C=O), 1608, 1503, 1373 (C–N), 1230, 1192, 1108, 1036, 919, 851, 817, 730. ^{1}H NMR (500 MHz, Chloroform-d) δ 8.49 (s, 2H), 7.30 (s, 4H), 7.17 (t, 2H), 3.60 (d, 1H), 2.32 (s, 1H), 2.21 (d, 6H), 1.72 (s, 5H), 1.28 (s, 3H), 0.93 (s, 2H).

Other PI-H(2–4) were synthesized by the similar procedure as above.

PI-H2. Yield: 93%. FTIR (blade-coating film, cm^{-1}): ν = 2929 (CH_2–H), 1786 (C=O), 1731 (C=O), 1611, 1504, 1375 (C–N), 1256, 1192, 1108, 1036, 984, 877, 724. ^{1}H NMR (500 MHz, Chloroform-d) δ 8.05 (d, 2H), 7.99–7.86 (m, 4H), 7.30 (s, 4H), 7.14 (d, 2H), 3.57 (d, 1H), 2.22 (s, 6H), 2.14 (d, 1H), 1.72 (s, 5H), 1.23 (s, 3H), 0.91 (d, 2H).

PI-H3. Yield: 96%. FTIR (blade-coating film, cm^{-1}): ν = 2928 (CH_2–H), 1779 (C=O), 1723 (C=O), 1609, 1504, 1374 (C–N), 1275, 1103, 895, 812, 748. ^{1}H NMR (500 MHz, Chloroform-d) δ 8.01 (d, 2H), 7.56 (d, 2H), 7.49 (d, 2H), 7.28 (s, 4H), 7.14 (d, 2H), 3.56 (d, 1H), 2.21 (s, 6H), 2.13 (d, 1H), 1.72 (s, 5H), 1.28–1.23 (m, 3H), 0.92–0.87 (m, 2H).

PI-H4. Yield: 94%. FTIR (blade-coating film, cm^{-1}): ν = 2928 (CH_2–H), 1777 (C=O), 1721 (C=O), 1620, 1504, 1373 (C–N), 1232, 1103, 890, 743. ^{1}H NMR (500 MHz, Chloroform-d) δ 8.26 (s, 2H), 8.10 (t, 4H), 7.31 (s, 4H), 7.18 (d, 2H), 3.59 (d, 1H), 2.23 (s, 6H), 2.20–2.15 (m, 1H), 1.72 (s, 5H), 1.26 (d, 3H), 0.94–0.87 (m, 2H).

PI-H5. Yield: 96%. FTIR (blade-coating film, cm^{-1}): ν = 2927 (CH_2–H), 1779 (C=O), 1726(C=O), 1618, 1503, 1375 (C–N), 1296, 1208, 1105, 980, 861, 820, 726. ^{1}H NMR (500 MHz, Chloroform-d) δ 8.27 (d, 2H), 8.13 (d, 4H), 7.30 (s, 4H), 7.16 (d, 2H), 3.58 (d, 1H), 2.31 (s, 1H), 2.22 (s, 6H), 1.72 (s, 5H), 1.28 – 1.23 (m, 3H), 0.93–0.89 (m, 2H).

Low-temperature two-step method. As comparison, these PIs were also prepared by a low-temperature two-step method (denoted as PI-L(1–5)) as shown in Figure 2. The synthesis of PI-L1 was used as a typical example. 1.5423 g (5 mmol) CHMBMA and 13 mL dry NMP were added into a 100 mL three-necked flask and stirred at room temperature under N_2 atmosphere. Then 1.0906 g (5 mmol) PMDA was added into the above flask and kept stirring for 24 h to form a viscous solution of poly(amic acid) (PAA). Finally, 1.5 mL pyridine and 3 mL acetic anhydride were added into the PAA solution and kept stirring for another 24 h to finish the chemical imidization. The viscous yellow solution was diluted by 30 mL chloroform and poured slowly into 500 mL methanol under the vigorous stirring to give some white fiber-like precipitate. PI-L1 was collected by filtration and dried at 150°C in vacuum oven for 24 h. It was purified by reprecipitating twice. Yield: 96%. FTIR (blade-coating film, cm^{-1}): ν = 2928 (CH_2–H), 1779 (C=O), 1729 (C=O), 1608, 1504, 1373 (C–N), 1230, 1193, 1108, 1036, 919, 851, 818, 730.

Other PI-L(2–4) were synthesized by the similar procedure as above.

PI-L2. Yield: 94%. FTIR (blade-coating film, cm^{-1}): ν = 2929 (CH_2–H), 1786 (C=O), 1731 (C=O), 1611, 1504, 1375 (C–N), 1256, 1192, 1108, 1037, 984, 878, 724.

PI-L3. Yield: 93%. FTIR (blade-coating film, cm^{-1}): ν = 2928 (CH_2–H), 1779 (C=O), 1723 (C=O), 1609, 1504, 1373 (C–N), 1276, 1104, 895, 812, 748.

PI-L4. Yield: 94%. FTIR (blade-coating film, cm^{-1}): ν = 2928 (CH_2–H), 1777 (C=O), 1722 (C=O), 1620, 1504, 1373 (C–N), 1233, 1104, 890, 743.

PI-L5. Yield: 95%. FTIR (blade-coating film, cm^{-1}): ν = 2926 (CH_2–H), 1779 (C=O), 1725(C=O), 1618, 1502, 1374 (C–N), 1295, 1207, 1104, 979, 861, 820, 725.

Film preparation

The PI films were prepared by the blade-coating method with Elcometer 4340 Automatic Film Applicator. One of PIs was dissolved in fresh distilled DMAc to form a solution with a solid content of 15 wt% and then filtered by a 0.7 μm fiberglass syringe filter at room temperature. The homogeneous transparent PI solution was kept in oven at 60°C for 2 h. Afterward it was blade-coated on a clean glass substrate at 60°C with the blade height of 500 μm and the coating speed of 0.2 inches/second. The glass substrate with PI solution was kept at 60°C to evaporate DMAc for 4 h to form film. Subsequently, it was transferred into a vacuum oven and kept at 100°C/3 h, 150°C/3 h and 200°C/12 h to remove the residual solvent. Finally, the glass substrate was cooled to room temperature and immersed in deionized water to give a PI film.

Results and discussion

Monomer synthesis

The synthetic route of novel diamine CHMBMA is shown in Figure 1. With hydrochloric acid as the catalyst, cyclohexanecarbaldehyde was used as a linking group to bridge o-toluidine via the Mannich and rearrangement reactions to generate CHMBMA. The excessive amount of o-toluidine was served as the reaction medium without any other organic solvent. The chemical structure of

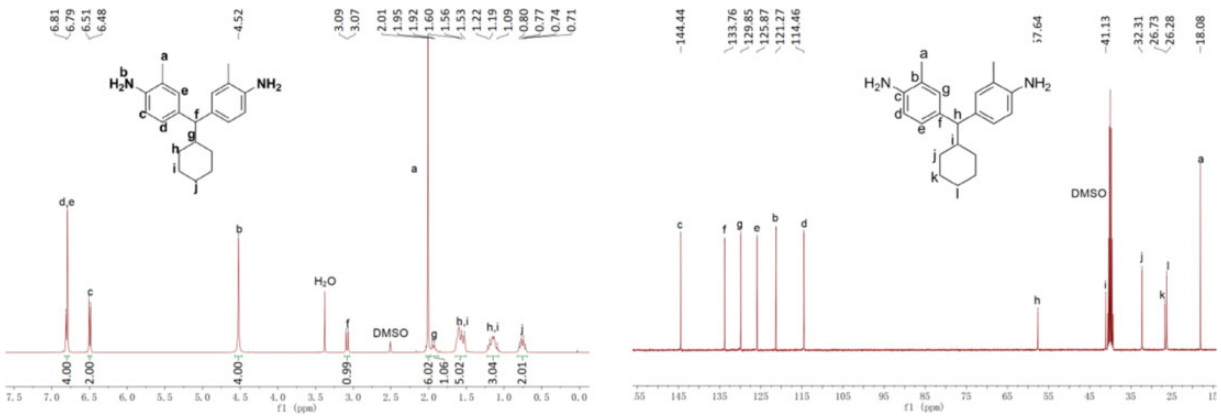

Figure 3. ^{1}H and ^{13}C NMR spectra of diamine CHMBMA.

CHMBMA was identified by ^{1}H NMR and ^{13}C NMR in deuterated dimethyl sulfoxide and the corresponding spectra were exhibited in Figure 3. From the ^{1}H NMR spectrum in Figure 3 (left), the signals of aromatic protons were observed in the range from 6.81 to 6.47 ppm. The peak at around 4.52 ppm was ascribed to the protons of amino groups. In addition, the peak at around 2.01 ppm was assigned to the protons of ortho-methyl and the peaks from 1.95 to 0.71 ppm were assigned to the protons of cyclohexyle. Meanwhile, from the ^{13}C NMR spectrum in Figure 3 (right), all the carbon signals of CHMBMA were found in the range of 18.08–144.44 ppm accordingly. Furthermore, the result of mass spectrometry measurements indicated that the molecular ion peak of CHMBMA was found at 309.2347, which was in accordance with the theoretical value of 309.2331 and further confirmed the chemical structure of CHMBMA. The result of DSC analysis displayed that the melting point of CHMBMA was around 121°C.

Polymer synthesis

As shown in Figure 2, PI-H(1–5) were prepared through the high-temperature one-step method with thermal imidization from CHMBMA with five commercial aromatic dianhydrides in m-cresol and catalytic amount of isoquinoline. As comparison, PI-L(1–5) were also prepared by the low-temperature two-step method in NMP with chemical imidization by using pyridine and acetic anhydride (1:2, volume ratio). The solid content was kept around 15 wt% in all polymerization processes. The resulting PIs were characterized by GPC, ^{1}H NMR, FTIR and elemental analysis measurements. From Table 1, the M_ws of PI-H(1–5) are in the range from 9.08×10^4 to 27.48×10^4 g mol^{-1} respectively with PDIs from 3.29 to 6.13, while the M_ws of PI-L(1–5) are in the range from 4.05×10^4 to 7.09×10^4 g mol^{-1} respectively with the PDIs from 3.53 to 4.35. Thus, the molecular weights of PIs from one-step method are higher that those from two-step method, which indicates that phenolic solvents might be beneficial to the increase of molecular weights of PIs.

Table 1. Molecular weights and PDIs of the resulting PIs.

PIs	$M_n \times 10^{-4}$ a)[g mol^{-1}]	$M_w \times 10^{-4}$ b)[g mol^{-1}]	PDI c)
PI-H1	7.98	27.48	3.44
PI-H2	2.76	9.08	3.29
PI-H3	5.63	20.23	3.59
PI-H4	2.59	9.40	3.63
PI-H5	1.61	9.88	6.13
PI-L1	1.54	5.52	3.59
PI-L2	1.63	7.09	4.35
PI-L3	1.12	4.43	3.97
PI-L4	1.15	4.05	3.53
PI-L5	1.55	5.49	3.54

a) M_n: number-averaged molecular weight; b) M_w: weight-averaged molecular weight; c) PDI: polydispersity index.

^{1}H NMR spectra of PI-H(1–5) were shown in SI Figure S1. All the peaks were labeled by English letters and ascribed to the corresponding protons, which confirmed their chemical structure. The FTIR spectra of PI-H(1–5) and PI-L(1–5) were exhibited in Figure 4. No significant difference was observed in the FTIR spectra of PI-H(1–5) and PI-L(1–5). All the typical absorption peaks belong to the imide rings of the resulting PIs were found at 1373–1375 cm^{-1} (C–N asymmetric stretching), 1777–1786 cm^{-1} (C=O asymmetrical stretching) and 1721–1731 cm^{-1} (C=O symmetrical stretching). On the other hand, the peaks in the range of 3220–3450 cm^{-1} (N–H stretching) almost disappeared, which indicated the imidization of the resulting PIs was finished completely. In addition, the elemental analysis data of PI-H(1–5) (SI Table S1) were nearly consistent with their corresponding theoretical values and further confirmed their chemical structures.

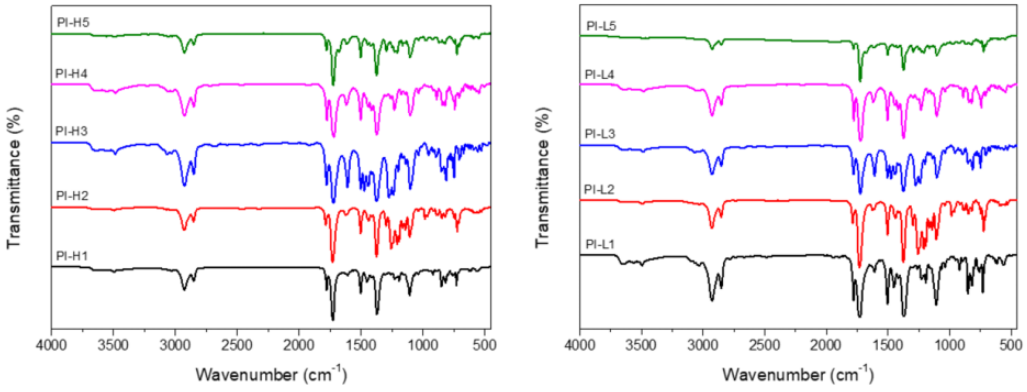

Figure 4. FTIR spectra of the resulting PIs.

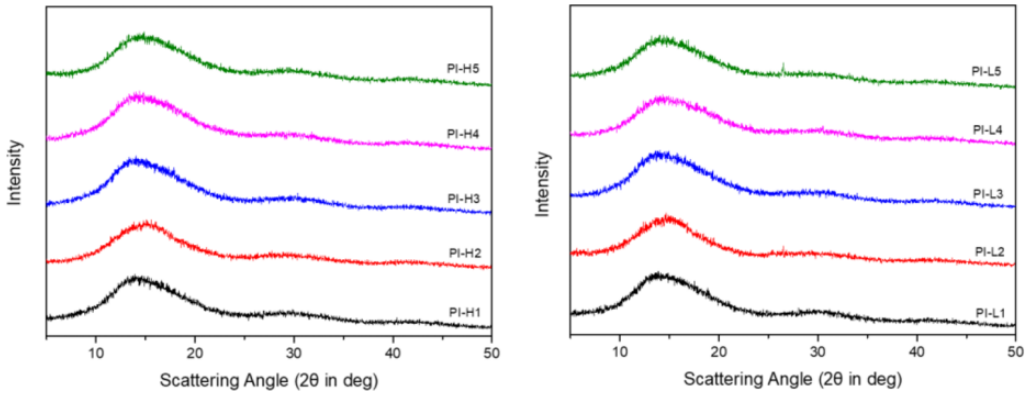

Figure 5. X-ray diffraction curves of the resulting PI films.

Table 2. Solubility and water absorption rates of PI-H(1–5).

PIs	DMF	DMAc	NMP	m-cresol	$CHCl_3$	THF	acetone	Water absorption [%]
PI-H1	+	+	+	+	+	+	−	1.72
PI-H2	+	+	+	+	+	+	+	0.99
PI-H3	+	+	+	+	+	+	−	0.67
PI-H4	+	+	+	+	+	+	−	2.45
PI-H5	+	+	+	+	+	+	−	1.38

DMF: N, N-dimethylformamide; DMAc: dimethylacetamide; NMP: *N*-methyl-2-pyrrolidone; $CHCl_3$: trichloromethane; THF: tetrahydrofuran; +: soluble; −: insoluble.

X-ray diffraction

The XRD diffraction curves of the resulting PI films were shown in Figure 5. There are no obvious difference in the XRD diffraction curves of PI-H(1–5) and PI-L(1–5), which indicated the polymerization method had little effect on the morphology of the resulting PIs. Only one main broad diffraction peak like a bread was observed for all PI films, which indicated they were amorphous polymers. The incorporation of pendant cyclohexyl and methyl into diamine units significantly reduced the packing density and increased the free volume of the resulting PIs. This was coincided with the good thermal stability, transparency and solubility of PI films.

Solubility

Generally, the solubility of polymers in organic solvents depends on their chain packing density abd intermolecular interactions, which are determined by the rigidity, symmetry and regularity of polymeric backbone. The solubility of the resulting PIs was measured by dissolving 10 mg of PIs in 1 mL of solvent at 30°C for 2 h. As demonstrated in Table 2, all the resulting PIs displayed outstanding solubility in organic solvents, especially in low boiling-point solvents such as $CHCl_3$ and THF. Moreover, PI-H2 showed much better solubility than that of other PIs, which was attributed to the presence of hexafluoroisopropyls

Table 3. Thermal properties and CTEs of the resulting PI films.

PIs	T_g [a] [°C]	T_g [b] [°C]	$T_{5\%}$ [c] [°C]	CTE [d] [ppm °C^{-1}]
PI-H1	— [e]	450	473	59
PI-H2	323	345	479	83
PI-H3	319	336	474	84
PI-H4	361	387	480	64
PI-H5	320	340	466	85
PI-L1	—	436	470	52
PI-L2	319	338	475	84
PI-L3	312	324	470	63
PI-L4	349	365	471	56
PI-L5	316	335	469	80

[a] T_g: glass transition temperature, evaluated by DSC; [b] T_g: glass transition temperature, evaluated by DMA; [c] $T_{5\%}$: temperature at 5% weight loss; [d] CTE: coefficient of thermal expansion; [e] Not detected.

Table 4. Mechanical behaviors of the resulting PI films.

PIs	Film thickness [μm]	Tensile strength [MPa]	Tensile modulus [GPa]	Elongation at break [%]
PI-H1	70	97.6	1.5	12.8
PI-H2	65	73.5	1.9	5.9
PI-H3	75	95.3	0.9	14.9
PI-H4	60	85.0	1.3	9.4
PI-H5	70	74.5	1.5	6.5
PI-L1	55	91.6	1.0	14.5
PI-L2	55	72.2	1.3	7.5
PI-L3	50	86.3	1.3	8.9
PI-L4	60	75.4	1.5	7.4
PI-L5	60	83.4	1.3	10.2

(–C(CF$_3$)$_2$–) to increase the flexibility and affinity of its main chains and even make it soluble in acetone at room temperature. In short, the incorporation of pendant cyclohexyl and side methyl into PI backbone can effectively enhance the solubility in organic solvents by weakening the cohesion and close-packing of PI main chains.

Water absorption rate

The water absorption rates of PI-H(1–5) films were investigated at room temperature and the data were summarized in Table 2. The water absorption rates of PI-H(1–5) films were in the range from 0.99 to 2.45%, which were lower than that of the commercial Kapton film (3.1%).[34]

Thermal properties

The thermal properties of the resulting PIs were investigated by DSC, TGA and DMA measurements under N_2 atmosphere. The DSC and DMA curves of the PIs were displayed in SI Figure S2, and the corresponding T_g values were listed in Table 3. All the T_gs of the resulting PIs were higher than 300°C, which were measured by DSC (312–361°C except for PI-H1 and PI-L1) or DMA (335–450°C). The T_gs obtained by DMA were slightly higher than those by DSC, but both variation trends were matched well with each other. Moreover, the T_gs of PI-H(1–5) were slightly higher than the corresponding ones of PI-L(1–5), which may be ascribed to the relatively higher molecular weights of PI-H(1–5) prepared by the high-temperature one-step method. Especially, the T_g of PI-H1 was not detected before 400°C by DSC measurement, but it reached 450°C by DMA measurement, which was the highest one among them and attributed to its most rigid backbone. Even for PI-H3 with a flexible ether linkage in dianhydride unit, its T_g still reached 319°C (by DSC) and 336°C (by DMA), which indicated that the introduction of ortho-methyl and cyclohexyl did not reduce their thermal properties. Comparing to our previous work, the T_gs were enhanced when the ortho *tert*-butyl was replaced by the ortho-methyl.[34] At the same time, the solubility of PIs was remained fairly and the cost could be reduced.

The thermal stability of the resulting PIs was evaluated by TGA under nitrogen atmosphere and the TGA curves were illustrated in SI Figure S3. In addition, the temperatures of 5% weight loss ($T_{5\%}$) were listed in Table 3. All the PIs exhibited good thermal stability and their $T_{5\%}$s were in the range of 466–480°C. This indicated that the introduction of ortho-methyl and cyclohexyl groups did not sacrifice their inherent thermal stability.

The thermal-dimensional stability of PI-H(1–5) and PI-L(1–5) films was evaluated by TMA and the coefficients of thermal expansion (CTE) were summarized in Table 3. The CTE values of PI-H(1–5) and PI-L(1–5) films were in the range from 52 to 85 ppm °C^{-1}, which were similar as the level of common transparent flexible polymer systems.[36] Generally, PIs with the highly rigid main chains possess the low CTE values due to the large packing density.[30,37] Moreover, the low CTE values of PIs are also dominated by the degree of molecular in-plane orientation.[38,39] Here, the introduction of cyclohexyl and methyl groups into PIs enhanced their molecular mobility and resulted in the relatively high CTE values. Among them, the CTE value of PI-H1 was the lowest one due to its most rigid molecular structure of PMDA.

Mechanical behaviors

The mechanical properties of the resulting PI films were measured by tensile testing at room temperature and the results were outlined in Table 4. Their tensile strength values were in the range of 72.2–97.6 MPa, together with the tensile modulus values of 0.9–1.9 GPa and the elongation at break of 5.9–14.9%, which indicated all the resulting PI films were tough and flexible.

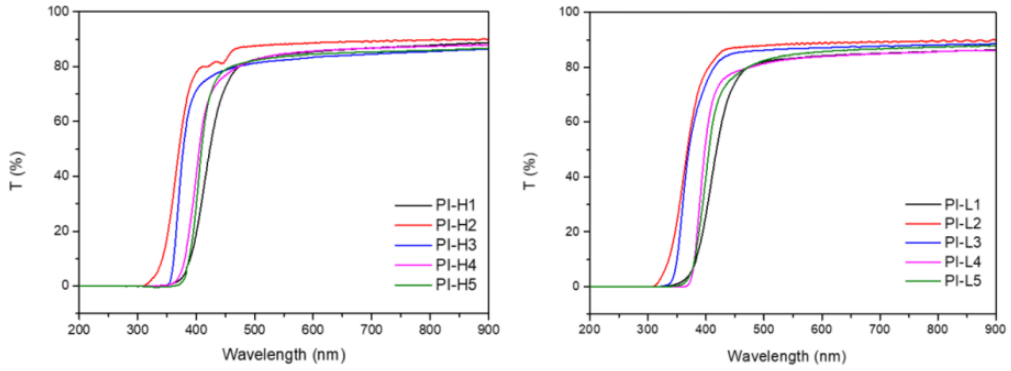

Figure 6. UV-vis spectra of the resulting PI films (thickness: 20–26 μm).

Table 5. Optical performance of the resulting PI films.

PIs	Film thickness [μm]	T_{vis} [a] [%]	T_{450} [b] [%]	T_{400} [c] [%]	λ_0 [d] [nm]
PI-H1	22	80	73	19	333
PI-H2	20	87	82	78	310
PI-H3	26	82	79	71	347
PI-H4	22	82	77	40	337
PI-H5	25	81	77	29	364
PI-L1	24	80	74	26	327
PI-L2	23	88	87	78	304
PI-L3	21	86	85	74	318
PI-L4	20	82	78	54	363
PI-L5	23	82	77	40	330

[a]The average transmittance in the visible light range (400–760 nm); [b]Transmittance at 450 nm; [c] Transmittance at 400 nm; [d] UV cut-off wavelength.

Optical performance

The optical performance of the resulting PI films (Thickness: 20–26 μm) was studied by UV-Vis spectrometer. Their UV-vis spectra were displayed in Figure 6 and the results were listed in Table 5. The average transmittance of these PI films in the visible light range (400–760 nm) was above 80%. Moreover, their cut-off wavelengths were between 304 and 364 nm. Comparing the optical performance of PI-H(1–5) and PI-L(1–5), no obvious difference was observed among them. In the visible region, PI-H2 and PI-L2 exhibited the highest average transmittance (87–88%). This is ascribed to the trifluoromethyls in 6FDA, which provide steric hindrance and high electronegativity of C–F bonds to inhibit the formation of CTC.[6,13] On the contrary, PI-H1 and PI-L1 possessed the lowest average transmittance (80%) due to the most rigid dianhydride PMDA, but still better than that of Kapton (69%).[16]

The optical photographs of the resulting PI films (Thickness: 55–65 μm) were shown in Figure 7. All the PI films had good transparence with the different degree of light yellow, which was depended on the used dianhydride. The film color of PI-L(1–5) was relatively lighter than the corresponding one of PI-H(1–5), which indicated that the high temperature in the polymerization process had a negative effect on the colorlessness of the resulting PI films.[29,40]

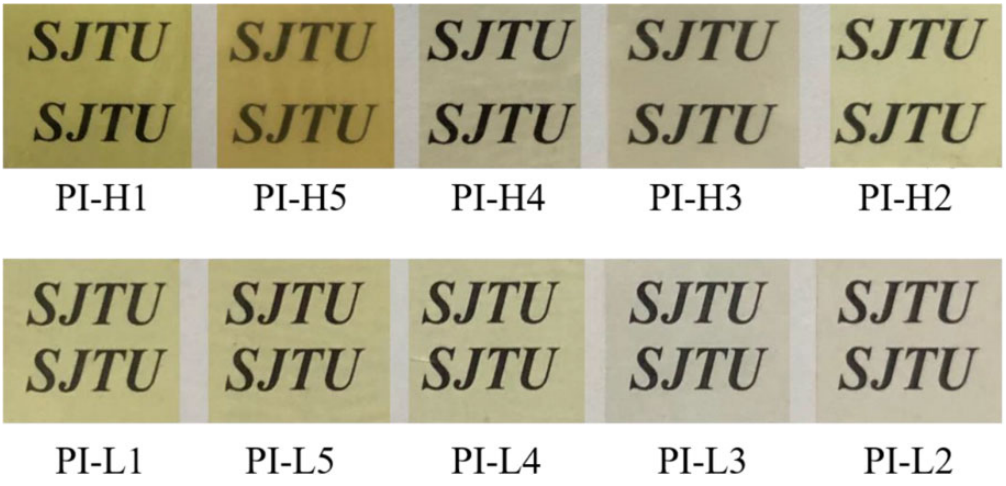

Figure 7. Optical photographs of the resulting PI films (Thickness: 55–65 μm).

Conclusions

In this work, a novel diamine containing cyclohexyl and ortho-methyl groups were successfully synthesized and then polymerized with five commercial dianhydrides via different methods. The resulting PIs exhibited outstanding solubility in various organic solvents, such as $CHCl_3$ and THF. Meanwhile, their corresponding films displayed excellent mechanical behaviors, high thermal stability (T_g > 312°C, $T_{5\%}$ > 466°C) and good optical properties (T_{vis} > 80%). The M_ws of PI-L(1–5) were lower than those of PI-H(1–5), but the film color of PI-L(1–5) is relatively lighter than the corresponding one of PI-H(1–5). In summary, the introduction of cyclohexyl and ortho-methyl groups into PI chains is an effective way to enhance their solubility and transparency without decreasing their thermal stability. These transparent PI films have potential applications in the optical-electronic devices.

Declaration of conflicting interests

The author(s) declared no potential conflicts of interest with respect to the research, authorship, and/or publication of this article.

Funding

The author(s) disclosed receipt of the following financial support for the research, authorship, and/or publication of this article: This work was supported by Science and Technology Commission of Shanghai Municipality Basic Research Project (No. 16JC1403600), Equipment Research and Development Sharing Technology Project (No. 41421060301).

ORCID iD

Wei Huang https://orcid.org/0000-0002-7885-4378

Supplemental material

Supplemental material for this article is available online.

References

1. Ji D, Li T, Hu W, et al. Recent progress in aromatic polyimide dielectrics for organic electronic devices and circuits. *Adv Mater* 2019; **31**: 1806070.
2. Huang W, Yan D and Lu Q. Synthesis and characterization of a highly soluble aromatic polyimide from 4,4′-methylene-bis(2-tert-butylaniline). *Macromol Rapid Commun* 2001; **22**: 1481–1484.
3. Wu X, Jiang G, Zhang Y, et al. Enhancement of flame retardancy of colorless and transparent semi-alicyclic polyimide film from hydrogenated-BPDA and 4,4′-oxydianiline via the incorporation of phosphazene oligomer. *Polymers* 2020; **12**: 90.
4. Zhuang Y, Jong GS and Lee YM. Polyimides containing aliphatic/alicyclic segments in the main chains. *Prog Polym Sci* 2019; **92**: 35–88.
5. Zhang Q, Tsai CY, Li LJ, et al. Colorless-to-colorful switching electrochromic polyimides with very high contrast ratio. *Nat Commun* 2019; **10**: 1–8.
6. Jeong KM, Tapaswi PK, Kambara T, et al. Photoconductive polyimides derived from a novel imidazole-containing diamine. *High Perform Polym* 2019; **32**: 620–630.
7. Yang Y, Jung Y, Cho MD, et al. Transient color changes in oxidative-stable fluorinated polyimide film for flexible display substrates. *RSC Adv* 2015; **5**: 57339–57345.
8. Zhang Y, Tan Y-Y, Liu J-G, et al. Molecular design, synthesis and characterization of intrinsically black polyimide films with high thermal stability and good electrical properties. *J Polym Res* 2019; **26**: 1–10.
9. Zhou Z, Zhang Y, Liu S, et al. Flexible and highly fluorescent aromatic polyimide: design, synthesis, properties, and mechanism. *J Mater Chem C* 2016; **4**: 10509–10517.
10. Hasegawa M and Horie K. Photophysics, photochemistry, and optical properties of polyimides. *Prog Polym Sci* 2001; **26**: 259–335.
11. Liaw DJ, Wang KL, Huang YC, et al. Advanced polyimide materials: syntheses, physical properties and applications. *Prog Polym Sci* 2012; **37**: 907–974.
12. Liu H, Zhai L, Bai L, et al. Synthesis and characterization of optically transparent semi-aromatic polyimide films with low fluorine content. *Polymer* 2019; **163**: 106–114.
13. Lang Y, Huang W and Yan D. Polyimides with side groups: synthesis and effects of side groups on their properties. *J Polym Sci A Polym Chem* 2016; **55**: 533–559.
14. Tapaswi PK, Choi MC, Jeong KM, et al. Transparent aromatic polyimides derived from thiophenyl-substituted benzidines with high refractive index and small birefringence. *Macromolecules* 2015; **48**: 3462–3474.
15. Li C, Yi L, Xu S, et al. Synthesis and characterization of polyimides from 4,4′-(3-(tert-butyl)-4-aminophenoxy)diphenyl ether. *J Polym Res* 2017; **24**: 1–9.
16. Wu Q, Ma X, Zheng F, et al. Synthesis of highly transparent and heat-resistant polyimides containing bulky pendant moieties. *Polym Int* 2019; **68**: 1186–1193.
17. Ni HJ, Liu JG, Wang ZH, et al. A review on colorless and optically transparent polyimide films: chemistry, process and engineering applications. *J Ind Eng Chem* 2015; **28**: 16–27.
18. Revathi R, Prabunathan P, Devaraju S, et al. Synthesis of soluble polyimides based on ether-linked cyclohexyldiamine and their ultraviolet shielding behavior. *High Perform Polym* 2015; **27**: 247–253.
19. Huang X, Huang W, Yan D, et al. Synthesis and characterization of thioether-containing polyimides with high refractive indices. *J Polym Res* 2012; **19**: 1–9.
20. Zhang SJ, Bu QQ, Li YF, et al. High organosolubility and optical transparency of novel polyimides derived from 2′,7′-bis(4-amino-2-trifluoromethylphenoxy)-spiro(fluorene-9,9′-xanthene). *Mater Chem Phys* 2011; **128**: 392–399.
21. Hasegawa M, Ishigami T and Ishii J.Optically transparent aromatic poly(ester imide)s with low coefficients of thermal

expansion (1). Self-orientation behavior during solution casting process and substituent effect. *Polymer* 2015; **74**: 1–15.
22. Liu Y, Zhou Z, Qu L, et al. Exceptionally thermostable and soluble aromatic polyimides with special characteristics: intrinsic ultralow dielectric constant, static random access memory behaviors, transparency and fluorescence. *Mater Chem Front* 2017; **1**: 326–337.
23. Tapaswi PK, Choi MC, Nagappan S, et al. Synthesis and characterization of highly transparent and hydrophobic fluorinated polyimides derived from perfluorodecylthio substituted diamine monomers. *J Polym Sci A Polym Chem* 2015; **53**: 479–488.
24. Kim SD, Lee S, Heo J, et al. Soluble polyimides with trifluoromethyl pendent groups. *Polymer* 2013; **54**: 5648–5654.
25. Yeo H, Goh M, Ku B-C, et al. Synthesis and characterization of highly-fluorinated colorless polyimides derived from 4,4′-((perfluoro-[1,1′-biphenyl]-4,4′-diyl)bis(oxy))-bis(2,6-dimethylaniline) and aromatic dianhydrides. *Polymer* 2015; **76**: 280–286.
26. Jang W, Lee H-S, Lee S, et al. The optical and dielectric characterization of light-colored fluorinated polyimides based on 1,3-bis(4-amino-2-trifluoromethylphenoxy)benzene. *Mater Chem Phys* 2007; **104**: 342–349.
27. Kim SD, Kim SY and Chung IS. Soluble and transparent polyimides from unsymmetrical diamine containing two trifluoromethyl groups. *J Polym Sci A Polym Chem* 2013; **51**: 4413–4422.
28. Yi C, Li W, Shi S, et al. High-temperature-resistant and colorless polyimide: preparations, properties, and applications. *Sol Energy* 2020; **195**: 340–354.
29. Tapaswi PK and Ha CS. Recent trends on transparent colorless polyimides with balanced thermal and optical properties: design and synthesis. *Macromol Chem Phys* 2019; **220**: 1800313.
30. Jiang GL, Wang DY, Du HP, et al. Reduced coefficients of linear thermal expansion of colorless and transparent semi-alicyclic polyimide films via incorporation of rigid-rod amide moiety: preparation and properties. *Polymers* 2020; **12**: 413.
31. Abajo JD and Campa JGD. Processable aromatic polyimides. *Adv Polym Sci* 1999; **140**: 23–59.
32. Ghaemy M and Alizadeh R. Synthesis of soluble and thermally stable polyimides from unsymmetrical diamine containing 2,4,5-triaryl imidazole pendent group. *Eur Polym J* 2009; **45**: 1681–1688.
33. Yao J, Wang C, Zhao X, et al. Highly transparent and soluble polyimides with synergistic effects of pyridine and cyclohexane. *High Perform Polym* 2018; **30**: 418–426.
34. Wu X, Shu C, He X, et al. Optically transparent and thermalstable polyimide films derived from a semi-aliphatic diamine: synthesis and properties. *Macromol Chem Phys* 2020; **221**: 1900506.
35. Bong S, Yeo H, Goh M, et al. Synthesis and characterization of colorless polyimides derived from 4-(4-aminophenoxy)-2,6-dimethylaniline. *Macromol Res* 2016; **24**: 1091–1097.
36. Hasegawa M, Kasamatsu K and Koseki K. Colorless poly(ester imide)s derived from hydrogenated trimellitic anhydride. *Eur Polym J* 2012; **48**: 483–498.
37. Lin SH, Li F, Cheng S, et al. Organo-soluble polyimides: synthesis and polymerization of 2,2′-bis(trifluoromethyl)-4,4′,5,5′-biphenyltetracarboxylic dianhydride. *Macromolecules* 1998; **31**: 2080–2086.
38. Song G, Wang D, Zhao X, et al. Synthesis and properties of polyimides-containing benzoxazole units in the main chain. *High Perform Polym* 2013; **25**: 354–360.
39. Hasegawa M. Semi-aromatic polyimides with low dielectric constant and low CTE. *High Perform Polym* 2001; **13**: S93–S106.
40. Matsumoto T, Ishiguro E and Komatsu S. Low temperature film-fabrication of hardly soluble alicyclic polyimides with high T_g by a combined chemical and thermal imidization method. *J Photopolym Sci Technol* 2014; **27**: 167–171.